ACS Catalysis

pubs.acs.org/acscatalysis Viewpoint

Critical Practices in Rigorously Assessing the Inherent Activity of Nanoparticle Electrocatalysts

Sean T. Dix, Shawn Lu, and Suljo Linic*

Cite This: *ACS Catal.* 2020, 10, 10735–10741 Read Online

ACCESS | Metrics & More | Article Recommendations | Supporting Information

Over past decades, much work has been done in developing novel electrocatalysts for various electrochemical reactions, including hydrogen oxidation, oxygen reduction, CO_2 reduction, water oxidation, and N_2 reduction. Various monometallic, bimetallic, core@shell, noble metal and noble-metal free materials, in many nanoscopic form factors (e.g., nanoparticles of different shapes and sizes, planar structures, etc.) have been studied in an effort to improve electrocatalyst activity while reducing cost.[1−3] While this focus on different materials, in terms of their composition and their form factors, has brought a great deal of excitement to the field, it has become increasingly difficult to rigorously assess the critical figures of merit that can compare these different materials, even on a relative scale.[4,5] In this viewpoint, we briefly discuss the figures of merit used to evaluate electrocatalysts, outline potential issues that have caught our attention as sometimes mishandled in published literature, and describe some useful practices that ensure rigorous assessment of inherent electrocatalytic activity of materials. To illustrate our central points, we use electrochemical oxygen reduction reaction (ORR) as an example. We note that our goal is not to provide a comprehensive review of the field. Rather, it is to present a *viewpoint* on a small sliver of the fast-developing field and to hopefully direct the field in the direction of a more rigorous evaluation of the performance of electrocatalytic materials. While we focus on ORR on Pt-based materials, we stress that the same level of rigor must be implemented when analyzing any electrochemical transformations and that, depending on the reactions or the material, this might require very different approaches.

ELECTROCATALYTIC ACTIVITY AS A FIGURE OF MERIT

There are several critical "figures of merit", which are commonly used to assess the activity of electrocatalysts. Specific activity ($j_k(V)$), which is defined as the potential-dependent net kinetic current (i_k) normalized by the electrochemically active surface area (ECSA, expressed in units of mA/cm^2), represents a measure of the surface activity of an electrocatalyst material. This is a critical metric that allows us to rigorously assess and compare the inherent activities of different materials. In our view, if the subject of a research effort is to study intrinsic electrocatalytic activity of a material or the mechanism of electrochemical reactions on an electrocatalyst surface, specific activity is the most important figure of merit that should always be reported. We note that, if not all surface sites are active, as is the case for carbon-based electrocatalysts, then in order to obtain relevant kinetic information, the kinetic currents must be normalized by the number of active sites. Rigorously counting the active sites is a significant problem that, for most materials, has not been adequately solved. The **mass activity**, which is the net kinetic current normalized by the mass of the electrocatalyst (generally reported as $A/mg_{catalyst}$) and the **volumetric activity** (the net kinetic current normalized by the volume occupied by the electrocatalyst) are not only a function of the inherent activity of the material's surface (the specific activity) but also of the form factor that the material takes. For example, larger nanoparticles will have lower mass and volumetric activity than smaller nanoparticles, for an identical material with identical specific activity. While the mass and volumetric activities can be important for the technoeconomic evaluation of an electrocatalyst in a device (such as a fuel cell), these two metrics are less useful when reporting the inherent activity of a material due to the above-mentioned impact of the form factors on these metrics. Another figure of merit that is often used in the literature is the **half-wave potential,** defined as the potential where one-half of the mass transport-limiting current is reached.[6] The half-wave potential can be used to compare the inherent activities of different materials, only if its measurement is based on properly normalizing for the effect of the ECSA. Comparing the half-wave potential (not normalized for the impact of ECSA) of two materials that have very different surface areas exposed to electrolyte should not be used to assess the relative electrochemical activity of these materials, since higher ECSA of a material compensates for a poor inherent activity. Our random sampling of 20 recently published papers in the field of ORR electrocatalysis that used half-wave potential to assess the activity of a material found that 11 did not account for the impact of different surface areas of the materials that were tested.

Received: July 10, 2020
Published: August 26, 2020

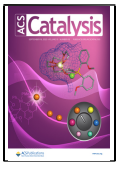

https://dx.doi.org/10.1021/acscatal.0c03028
ACS Catal. 2020, 10, 10735–10741

MEASURING ELECTROCATALYST ACTIVITY USING ROTATING DISK ELECTRODES

Typically, these figures of merit, including the specific activity, are measured using a rotating disk electrode (RDE) setup. In one version of the measurement, the electrocatalyst activity is studied by creating a flat nonporous electrode of the electrocatalytic material, such as a polycrystalline or single crystal metal or metal alloy surface. For ORR measurements, this flat RDE is placed in an oxygen-saturated electrolyte at a set rotation speed (often 1600 rpm) and connected to a reference and counter electrode. Current−potential ($I-V$) curves are collected as a function of the voltage of the working electrode (and, therefore, the electrocatalyst potential), and usually reported on the reversible hydrogen electrode (RHE) scale. An example of data obtained on a flat RDE of polycrystalline Pt in ORR is shown in Figure 1. The data

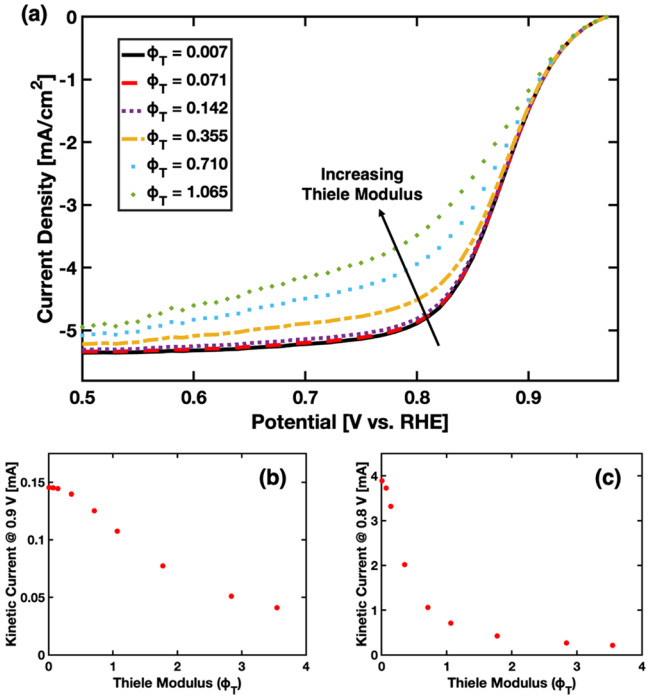

Figure 1. (a) RDE linear sweep voltammograms for a Pt-poly electrode in oxygen-saturated 0.1 M NaOH at 1600 rpm. An effectiveness factor (EF) model is imposed on the data to simulate the effects of various Thiele moduli (ϕ_{Th}). As the value of ϕ_{Th} increases, the electrode requires a greater overpotential to reach the mass-limiting current. (b, c) Effects of ϕ_{Th} on the kinetic current measured at 0.9 V vs RHE (panel (b)) and at 0.8 V vs RHE (panel (c)), using a model from the literature that has been detailed in the Supporting Information.

analysis in these systems is commonly based on the Koutecky−Levich approach, which assumes that there are two potential-dependent regimes that control the appearance of the $I-V$ curves. At high overpotential, the measured current is controlled by the rate of external mass transport of reactants (in ORR, it is O_2) from the bulk of the electrolyte to the electrocatalytically active layer on the RDE, while at low overpotentials, the reaction rate is controlled by the inherent net kinetic current of the active material (the net rate of the reactions taking place at the electrocatalyst surface). To separate the net kinetic current from the external mass transport limiting current, the total measured current is broken down using the Koutecky−Levich equation:

$$i = \left(\frac{1}{i_k} + \frac{1}{i_m}\right)^{-1} \quad (1)$$

where i is the net current measured, i_k the net kinetic current, and i_m is the external mass transport limiting current. The mass transport limiting current (which is dependent on several factors, including the RDE rotation speed) can be extracted from the $I-V$ curve as the potential independent current at high overpotentials. For ORR on Pt surfaces, this is typically the current at ∼0.5 V vs RHE, where the reaction is almost completely controlled by the rate of oxygen transport from the bulk of liquid electrolyte to the electrocatalyst layer. For flat electrodes, the analysis allows us to rigorously evaluate the specific current by dividing the net kinetic current by the electrochemically active surface area (ECSA), which, in this case, is the geometric area of the electrode.

It is often not possible to have electrocatalytic materials in the polycrystalline or single-crystal form factors, and there is a practical need to compare the activity of materials structured in different nanoscopic form factors (different shapes and sizes of nanoparticles) deposited on a RDE. In this setup, a thin porous active layer of electrocatalyst (usually electrocatalyst nanostructures are mixed with a porous carbon such as carbon black) is supported on an inert "non-porous" electrode (such as glassy carbon). This setup is known as the thin-film rotating disc electrode (TF-RDE).

The $I-V$ data obtained in the TF-RDE setup is also analyzed using the Koutecky−Levich equation. We note that, before applying the Koutecky−Levich analysis, all currents must be corrected for the capacitive current caused by the electrochemical double layer. This can be very important when high-surface-area supports (like carbon black) are used to support the active nanoparticle electrocatalysts. In these systems, electrical charging of the double layer can greatly alter the $I-V$ curve. One must be mindful that, in these systems, the reaction rate (i.e., the net measured current) is affected not only by the rate of external mass transport of reactants (in the case of ORR, it is O_2) from the electrolyte bulk to the surface of the outmost electrocatalyst layer and the net kinetic reaction rates, but also by the internal diffusion limitations from the outermost electrocatalyst layer to the electrochemically active sites, some of which are removed from that layer and reside inside the pores of the thin film.[7] We note that, for flat electrode surfaces discussed above, such as polycrystalline metallic plates, the internal diffusion limitations are non-existent, since all active sites are in the outermost electrocatalyst layer and therefore easily accessible to the reactants. On the other hand, for nanoscopic form factors where nanoparticles of different shapes are packed in the porous carbon material, these internal diffusion limitations, which affect the transport of reactants (such as O_2) to the active sites, can be significant and important.

The impact of internal diffusion limitations on the measured reaction rate can be described using the concept of an electrochemical effectiveness factor (EF). EF essentially represents the ratio of the measured net kinetic reaction rate to the rate that assumes no mass-transport limitations. While EF can be rigorously derived if certain assumptions are made about the pore geometry that the reactant must navigate

https://dx.doi.org/10.1021/acscatal.0c03028
ACS Catal. 2020, 10, 10735−10741

through the porous material to reach the active centers, EF generally takes the form of eq 2:

$$\mathrm{EF} = \frac{i_k}{i_{k,0}} = \frac{\tanh(\phi_{Th})}{\phi_{Th}} \quad (2)$$

where i_k and $i_{k,0}$ are the kinetic currents affected and unaffected by diffusion in the active electrocatalyst layer respectively, and ϕ_{Th} is the Thiele modulus. For low values of Thiele modulus ($\phi_{Th} < 0.1$), EF is close to 1, and for higher values of ϕ_{Th}, EF becomes increasingly smaller, asymptotically reaching $1/\phi_{Th}$. The Thiele modulus is controlled by several factors, including the active electrocatalyst layer depth (L), the diameter of the pores (D) that the reactants navigate in the active electrocatalyst layer (also affected by the packing density of the nanoparticles), the concentration (C_r) and diffusion coefficient (D_r) of the reactants and the reaction rate (j). As opposed to thermal catalytic systems and specific to electrochemical systems, the Thiele modulus is also dependent on the ohmic resistance (Ω) and ionic conductivity (σ) of the active layer:[8−10]

$$\phi_{Th} \approx f(L, D, C_r, D_r, j, \Omega, \sigma) \quad (3)$$

It is important to analyze how some of these parameters impact the Thiele modulus of an active electrocatalyst layer. For example, a thicker active porous layer with smaller pores and more crowded nanoparticles will increase the Thiele modulus and lower the measured kinetic current of the electrocatalyst. Conversely, larger pores (less crowding of the electrocatalyst particles) and thinner active layers will decrease the value of ϕ_{Th}. Furthermore, larger kinetic currents will also lead to a larger value of ϕ_{Th}, i.e., the effectiveness factor is a function of overpotential, and, for a given system, the effectiveness factor is smaller at larger overpotentials.

To demonstrate how ϕ_{Th} and EF can affect experimental $I-V$ curves, we applied eq 2 to a set of data that we obtained using a planar polycrystalline Pt electrode (which has no internal diffusion limitations, EF = 1; see the Supporting Information for more details) in electrochemical ORR. The data in Figure 1a show that an increase in ϕ_{Th}, which leads to a decrease in the EF of the electrocatalyst, results in the $I-V$ curves that have two characteristic differences, compared to the data unimpeded by the internal diffusion limitations. The differences are that, for systems with low EF, the slope of the $I-V$ curve in the region where the reactions rate (current) takes off is lower and the mass-transport limiting current is reached at larger overpotential. An inspection of published data suggests that these behaviors (low EF) are exhibited in many systems where various materials with different nanoscale form factors are studied and compared to each other, indicating that, in these studies, there were artifacts that resulted in internal diffusion limitations that compromised the results and conclusions. We note that the value of ϕ_{Th} is higher at higher overpotentials (higher currents), and therefore the EF value is lower and the deviation from the true kinetic current is greater, as shown in Figures 1b and 1c.

To avoid these internal diffusion limitations, it is recommended that electrocatalyst nanostructures are well-dispersed on a conductive porous support with an active layer film thickness of <0.1 μm in the TF-RDE setup.[11−13] While it is proposed that, under these conditions, a low ϕ_{Th} value can be achieved, one must be cognizant of the fact that ϕ_{Th} is effectively a dimensionless number that quantifies the ratio between kinetic reaction rates and internal diffusion rates.[8,14,15] As such, it is highly dependent on the particular geometry of the system (including the local packing of nanostructures and their shape), the size of the pores in the material that is packed on the TF-RDE, and the reactant and product diffusion constants in the electrolyte, as well as the rates of electrochemical reactions. Therefore, when comparing the electrochemical activity of different nanoscale form factors for different materials, it is important to assess the ϕ_{Th} values to ensure that the internal diffusion rates of reactants are not significantly impacting the results.

Although the accurate calculation of electrocatalyst activity can be compromised, because of slow diffusion in the active layer (low EF and large ϕ_{Th}) in TF-RDE as detailed above, we find that even greater misrepresentations of electrocatalyst activity originate from improper measurements of electrocatalyst surface area (ECSA). To obtain an accurate measure of specific electrocatalyst activity, the net kinetic current (i_k) must be normalized against an accurately measured ECSA of the electrocatalyst. Accurate measurements of ECSA are critical for assessing relevant activity of different materials and comparing their performance. Unfortunately, a random sampling of 20 recent papers on ORR electrocatalysis found that ~50% failed to properly normalize the kinetic current density against ECSA. In the following section, we describe experimental procedures used to accurately determine ECSA. Our focus is on Pt-based electrocatalysts, where electrochemical transformations occur on Pt surface sites. We note that comparing the activity of materials different than Pt requires a similar level of rigor for ECSA evaluations.

TECHNIQUES FOR CHARACTERIZING ECSA

Underpotential Deposition. One of the most common techniques for evaluating ECSA is underpotential deposition (UPD).[16] This is a voltammetric method in which the charge involved in electrochemically adsorbing/desorbing an adlayer of a selected chemical species is measured by integrating the area under the $I-V$ curve in the UPD region. For Pt group metals such as Pt, Ir, Ru, Rh, and Pd, atomic hydrogen can be used[17−21] whereas, for Ag, atomic lead (Pb) can be used.[22−24] Cu-UPD can also be used for a variety of metals, including Au, Pt, Ru, and Ag.[25,26]

For Pt-based electrocatalysts, hydrogen-underpotential deposition (H_{UPD}) is most commonly used to measure the ECSA. The Pt surface area is determined by integrating the $I-V$ curve from ~0.05 V to 0.4 V vs RHE under a suitable (non-adsorbing) electrolyte condition. This integration yields the charge associated with desorption of an underpotentially deposited adlayer of H (H_{UPD}) and can be converted to surface area through a conversion factor of 210 $\mu C/cm^2$ (the charge associated with electrochemical desorption of one H layer on a Pt surface).[27,28] We note that the dominant Pt facet will affect the conversion factor, necessitating precise nanoparticle characterization for the most accurate surface-area measurement.[5] To obtain accurate ECSA measurements from the current associated with the desorption of H_{UPD} through the integration of the $I-V$ curve, the background (noise) current (both potential dependent and independent) must be properly removed. Commonly, the potential-independent, double-layer capacitive current is assumed to be half of the difference between the limiting current of the anodic and cathodic sweeps between 0.4 and 0.5 V vs RHE. This is reflected in Figure 2 as the horizontal, dashed baseline from 0.05 V to 0.40 V vs RHE.

https://dx.doi.org/10.1021/acscatal.0c03028
ACS Catal. 2020, 10, 10735−10741

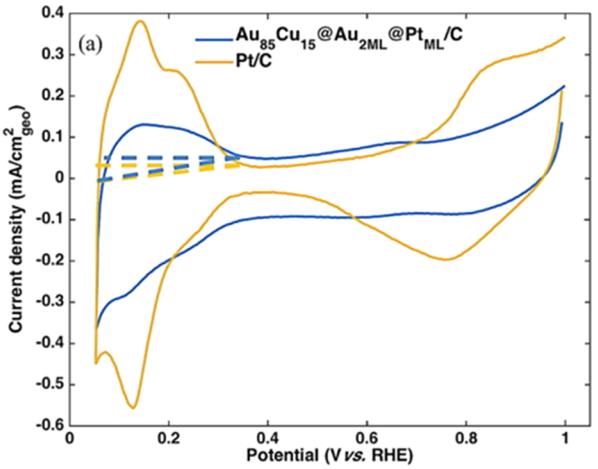

Figure 2. H_{UPD} analysis for a pure Pt (yellow) and Pt monolayer electrocatalyst (blue) developed within our group.[5] The H_{UPD} peak is integrated from 0.05 V to 0.40 V vs RHE, using either a constant or slanted baseline shown by the dotted lines. CV curves were obtained in Ar-saturated 0.1 M $HClO_4$, using a scan rate of 50 mV/s without electrode rotation. [Reprinted with permission from ref 29. Copyright 2017, Elsevier.]

The measured H_{UPD} desorption peak is then reduced by this amount, to remove contributions from the surface capacitance.[29] The background current can also include potential-dependent contributions (often related to the catalyst support effects), in addition to the constant capacitive current, leading to a potential-dependent baseline, rather than a horizontal baseline.[27,30,31] One way these potential-dependent currents can be taken into account is by using a slanted baseline, as shown by the dashed lines in Figure 2.[29] Using the horizontal baseline, rather than the sloped baseline, for the background subtraction can have a large effect on the measured ECSA. We demonstrated this in Figure 2, where we measured ECSA for a commercial, high-surface-area Pt/C electrocatalyst and a Pt monolayer core/shell electrocatalyst (Pt on Au/Cu alloy), deposited on carbon, developed in our laboratory. Using the sloped rather than horizontal baseline resulted in a measured ECSA increase of ~45% for the core/shell electrocatalyst, resulting in a dramatic decrease in calculated activity. A downside to this approach is that the choice of slope for the slanted baseline is somewhat subjective, leading to uncertainty in the measurement.

Another disadvantage of using the H_{UPD} method for surface-area calculations stems from the assumption that H_{UPD} atoms cover the entire electrocatalyst surface, which is most likely the case (based on extensive single crystal studies) for pure monometallic Pt samples but might not be the case for some Pt alloys. Changes in electrocatalyst electronic structure due to alloying can affect the adsorption energy of the H atoms and therefore can impact the H coverage.[28,32] For example, it was shown that $Pt_3Ni(111)$ does not adsorb a complete monolayer of H_{UPD}, resulting in sometimes erroneously low surface-area reports and artificially high specific-activity reports for this alloy.[33] To correct for this incomplete adsorption, modified ECSA calculation methods have been developed that account for the H_{UPD} coverage on the surface being <1, such as that described by eq 4:

$$\mathrm{ECSA} = \frac{Q_H}{\theta_H \times 210\ \mu\mathrm{C/cm}^2} \quad (4)$$

where Q_H is the charge associated with H_{UPD} desorption and θ_H is the hydrogen coverage. It is important to recognize that rigorous characterization of the surface coverage θ, under relevant electrochemical conditions, has not been widely adopted in the literature, with most reports in the literature assuming a value of unity for any Pt-tested Pt alloy.[34]

Carbon Monoxide (CO) Stripping. Because of the uncertainties associated with the H coverage on Pt alloy electrocatalysts, other voltammetric techniques, such as CO stripping, have been investigated.[28,35,36] In CO stripping experiments, an adlayer of CO is adsorbed on the electrocatalyst surface at reducing potentials (e.g., 0.05 V vs RHE for Pt surfaces) prior to the electrolyte being purged with an inert gas to remove any unbound CO. The potential is then swept to higher potentials and CO is oxidized from the surface. Similar to the H_{UPD} technique, the surface area can be determined by integrating the CO oxidation peak and converted to the ECSA by a conversion factor of 420 μC/cm^2 (i.e., this is a two-electron oxidation process).[28,37,38] One major advantage of CO stripping for ECSA characterization is that, on Pt alloys and pure Pt electrocatalysts, the saturation CO surface coverage has a tendency to be identical, which removes some degree of uncertainty present in the H_{UPD} method.[28,33] The baseline for integration (i.e., the background subtraction) can be viewed in the same way as for the H_{UPD} method. During the oxidation of CO in the anodic sweep, other currents, such as those associated with OH adsorption on the Pt surface and Pt-oxide formation, occur and must be corrected for. This can be accomplished by subtracting the anodic current measured post-stripping (when there is no longer CO on the surface) from the CO-stripping current. This operation yields only the net current associated with CO oxidation. Data in Figure 3 show the effect of background current subtraction on the measured current and, therefore, the measured ECSA. We note that the CO oxidation peak from 0.7 V to 0.8 V vs RHE is higher when the background current is not subtracted out (dashed line), compared to the peak when the background current is properly subtracted (solid line). The data in Figure 3

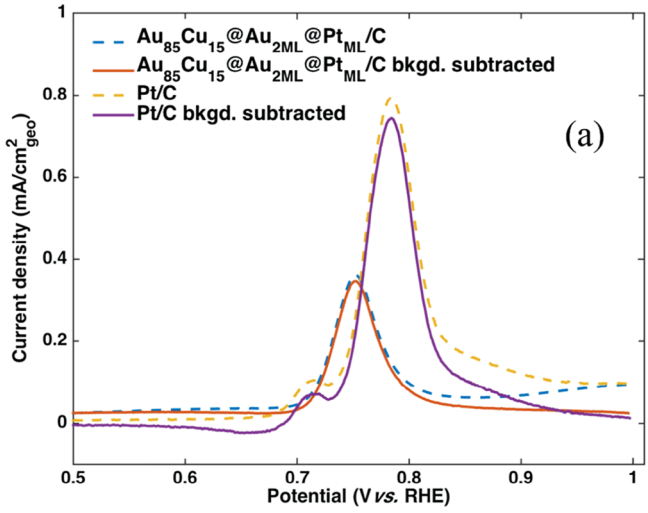

Figure 3. CO stripping voltammogram (scan rate = 10 mV/s) for Pt/C and Pt-monolayer electrocatalyst in an Ar-saturated 0.1 M $HClO_4$ electrolyte under no rotation. Raw currents are shown as dashed lines, while the background-subtracted currents are shown as solid lines. [Reprinted with permission from ref 29. Copyright 2017, Elsevier.]

https://dx.doi.org/10.1021/acscatal.0c03028
ACS Catal. 2020, 10, 10735−10741

show that, for the Au−Cu/Pt core−shell and Pt commercial standard electrocatalysts, the measured ECSA was reduced by ∼4% and ∼15%, respectively, when using the potential-dependent baseline to remove the background noise.

Baseline-Corrected H_{UPD} Measurements. The two techniques, H_{UPD} desorption and CO stripping, can be combined to give us more certainty in removing the background current in the H_{UPD} ECSA measurements for Pt electrocatalysts. The process involves saturating the Pt electrocatalyst surface with a layer of CO (holding potential at 0.05 V vs RHE). On this CO-poisoned Pt surface, the adsorption of H_{UPD} is prevented by the CO molecules. As the potential is increased from 0.05 V to 0.4 V, the background current in the H_{UPD} region, associated with the CO-poisoned Pt surface, is recorded. CO is then removed from the surface via CO oxidation and H can adsorb on the clean surface in subsequent scans. If we assume that CO is exclusively adsorbed on the Pt surface sites and that it blocks these sites against the H_{UPD} adsorption, then subtracting the CO poisoned scan from the CO-free scan in the H_{UPD} region yields the net current of the electro-oxidation of H_{UPD} free of background currents (potential-dependent and potential-independent), giving us a measure of the ECSA.

Figure 4 shows the specific activity of the commercial Pt standard and the Pt monolayer core/shell catalyst at 0.9 V vs RHE that we obtained using H_{UPD} (protocol 1 and 2), CO stripping (protocol 3 and 4), and the joint CO-stripping/H_{UPD} approach (protocol 5) to characterize ECSA. We note that, for these samples, the H_{UPD} protocols lead to specific activities 2.5−3 times higher than the CO-stripping protocols while the combined approach provides a specific activity in the middle between H_{UPD} and CO stripping. We find the combined technique (protocol 5) to be a good balance in the overestimation of ECSA from CO stripping and the underestimation of ECSA from the H_{UPD} method,[29] as seen in Figure 4. Ideally, a combination of methods would be reported to establish a range of electrocatalyst activities and assess the error.

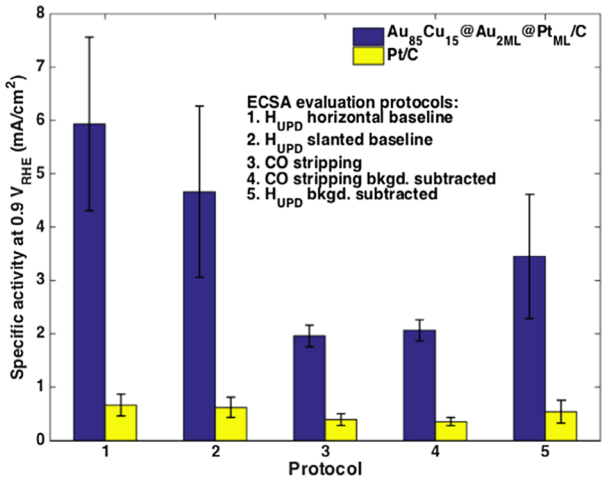

Figure 4. ORR specific activities for the different ECSA measuring protocols. Results for both the novel and standard Pt electrocatalyst are shown in blue and yellow, respectively. Error bars represent the standard deviation of the ECSA measurements. [Reprinted with permission from ref 29. Copyright 2017, Elsevier.]

Once the ECSA has been calculated, the specific activity can be produced simply by dividing the kinetic current by the ECSA at a particular overpotential. Typically, for a Pt surface, a working electrode potential of 0.9 V vs RHE is chosen. Mass and volumetric activities can then be calculated using the electrocatalyst loading and density. Half-wave potentials can be measured by regenerating the $I-V$ curve using the ECSA-normalized kinetic current density and the RDE area-normalized limiting current as shown in eq 5. The resulting $I-V$ curve will be the properly normalized current density versus applied potential and the accurate half-wave potential can be found.

$$j = \left(\frac{A_{ECSA}}{i_k} + \frac{A_{RDE}}{i_l} \right)^{-1} \quad (5)$$

The data in Figure 5 shows the impact of overestimated or underestimated ECSA on the normalized $I-V$ curves. As can be seen, the inaccuracies in the measurements of ECSA are manifested in shifting of the typical $I-V$ S-curve, with respect to the potential.

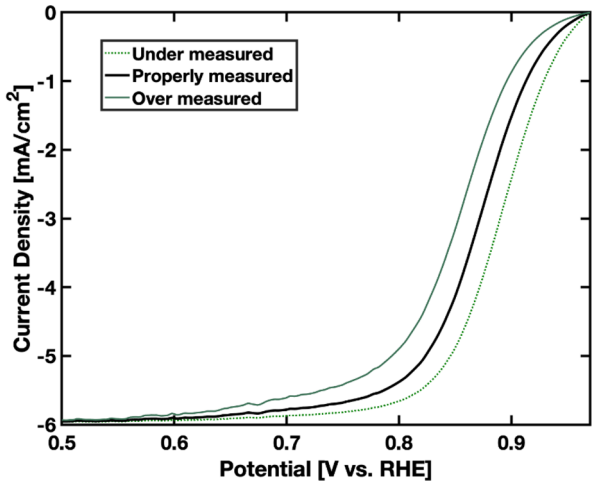

Figure 5. RDE linear sweep voltammograms for a Pt-poly electrode in oxygen-saturated 0.1 M NaOH at 1600 rpm. The black curve shows the properly normalized $I-V$ curve, using eq 5 (in the case of Pt-poly electrode, $A_{ECSA} = A_{RDE}$). The dotted green line represents a normalized $I-V$ curve derived if the magnitude of A_{ECSA} is underestimated to 50% of the real value, and the solid green line represents a normalized $I-V$ curve assuming a 2-fold overestimated A_{ESCA}.

CONCLUSION

Rigorous evaluation of activity of electrocatalysts is critical for the quantification of their absolute and relative performance. Unfortunately, the literature is full of examples of inaccurate assessment of electrocatalyst activity. These inaccuracies are amplified when very different materials are compared to each other (i.e., Pt versus carbon-based materials) or when different nanostructure form factors are used (i.e., solid nanoparticles versus nanocages, etc.). In this viewpoint, we discuss critical figures of merit for electrocatalyst activity, focusing on potential sources of error associated with quantifying the activity of nanostructured electrocatalysts. We show that internal diffusion limitations within a porous electrocatalysts support can impact the measurements. These diffusion

https://dx.doi.org/10.1021/acscatal.0c03028
ACS Catal. 2020, 10, 10735−10741

limitations can be quantified by an electrochemical effectiveness factor (EF) and the Thiele modulus (ϕ_{Th}). In addition, we discuss the importance of proper ECSA measurements on activity metrics. We present several techniques (i.e., H_{UPD}, CO stripping, and various combinations of the two techniques) to characterize the ECSA for monometallic Pt and Pt alloys.

■ ASSOCIATED CONTENT

Supporting Information

The Supporting Information is available free of charge at https://pubs.acs.org/doi/10.1021/acscatal.0c03028.

Oxygen reduction kinetic data on planar polycrystalline Pt electrode and electrochemical effectiveness factor modeling (PDF)

■ AUTHOR INFORMATION

Corresponding Author

Suljo Linic − *Department of Chemical Engineering and Michigan Catalysis Science and Technology Institute (MiCSTI), University of Michigan, Ann Arbor, Michigan 48109, United States;* orcid.org/0000-0003-2153-6755; Email: linic@umich.edu

Authors

Sean T. Dix − *Department of Chemical Engineering and Michigan Catalysis Science and Technology Institute (MiCSTI), University of Michigan, Ann Arbor, Michigan 48109, United States;* orcid.org/0000-0002-2880-8058

Shawn Lu − *Department of Chemical Engineering and Michigan Catalysis Science and Technology Institute (MiCSTI), University of Michigan, Ann Arbor, Michigan 48109, United States*

Complete contact information is available at: https://pubs.acs.org/10.1021/acscatal.0c03028

Notes

The authors declare no competing financial interest.

■ ACKNOWLEDGMENTS

The authors gratefully acknowledge support from the U.S. DOE Office of Basic Energy Sciences, Division of Chemical Sciences (Nos. FG-02-05ER15686 and DE-SC0021008) and the National Science Foundation (NSF) (Nos. CBET-1702471 and CHE 1800197).

■ REFERENCES

(1) Huang, X.; Zhao, Z.; Cao, L.; Chen, Y.; Zhu, E.; Lin, Z.; Li, M.; Yan, A.; Zettl, A.; Wang, Y. M.; Duan, X.; Mueller, T.; Huang, Y. High-Performance Transition Metal−Doped Pt3Ni Octahedra for Oxygen Reduction Reaction. *Science* **2015**, *348* (6240), 1230−1234.

(2) Wang, D.; Xin, H. L.; Hovden, R.; Wang, H.; Yu, Y.; Muller, D. A.; DiSalvo, F. J.; Abruña, H. D. Structurally Ordered Intermetallic Platinum−Cobalt Core−Shell Nanoparticles with Enhanced Activity and Stability as Oxygen Reduction Electrocatalysts. *Nat. Mater.* **2013**, *12* (1), 81−87.

(3) Cleve, T. V.; Moniri, S.; Belok, G.; More, K. L.; Linic, S. Nanoscale Engineering of Efficient Oxygen Reduction Electrocatalysts by Tailoring the Local Chemical Environment of Pt Surface Sites. *ACS Catal.* **2017**, *7* (1), 17−24.

(4) Watzele, S.; Hauenstein, P.; Liang, Y.; Xue, S.; Fichtner, J.; Garlyyev, B.; Scieszka, D.; Claudel, F.; Maillard, F.; Bandarenka, A. S. Determination of Electroactive Surface Area of Ni-, Co-, Fe-, and Ir-Based Oxide Electrocatalysts. *ACS Catal.* **2019**, *9* (10), 9222−9230.

(5) Wei, C.; Rao, R. R.; Peng, J.; Huang, B.; Stephens, I. E. L.; Risch, M.; Xu, Z. J.; Shao-Horn, Y. Recommended Practices and Benchmark Activity for Hydrogen and Oxygen Electrocatalysis in Water Splitting and Fuel Cells. *Adv. Mater.* **2019**, *31* (31), 1806296.

(6) Gasteiger, H. A.; Kocha, S. S.; Sompalli, B.; Wagner, F. T. Activity Benchmarks and Requirements for Pt, Pt-Alloy, and Non-Pt Oxygen Reduction Catalysts for PEMFCs. *Appl. Catal., B* **2005**, *56* (1), 9−35.

(7) Shih, Y.-H.; Sagar, G. V.; Lin, S. D. Effect of Electrode Pt Loading on the Oxygen Reduction Reaction Evaluated by Rotating Disk Electrode and Its Implication on the Reaction Kinetics. *J. Phys. Chem. C* **2008**, *112* (1), 123−130.

(8) Gloaguen, F.; Convert, P.; Gamburzev, S.; Velev, O. A.; Srinivasan, S. An Evaluation of the Macro-Homogeneous and Agglomerate Model for Oxygen Reduction in PEMFCs. *Electrochim. Acta* **1998**, *43* (24), 3767−3772.

(9) Lin, R.-B.; Shih, S.-M. Effects of Mass Transfer on Kinetics of Hydrogen Oxidation Reaction at Nafion/Pt-Black Thin-Film Electrodes. *J. Taiwan Inst. Chem. Eng.* **2013**, *44* (3), 393−401.

(10) Nam, J. H. Electrochemical Effectiveness Factors for Butler-Volmer Reaction Kinetics in Active Electrode Layers of Solid Oxide Fuel Cells. *J. Electrochem. Sci. Technol.* **2017**, *8* (4), 344−355.

(11) Garsany, Y.; Singer, I. L.; Swider-Lyons, K. E. Impact of Film Drying Procedures on RDE Characterization of Pt/VC Electrocatalysts. *J. Electroanal. Chem.* **2011**, *662* (2), 396−406.

(12) Ke, K.; Hiroshima, K.; Kamitaka, Y.; Hatanaka, T.; Morimoto, Y. An Accurate Evaluation for the Activity of Nano-Sized Electrocatalysts by a Thin-Film Rotating Disk Electrode: Oxygen Reduction on Pt/C. *Electrochim. Acta* **2012**, *72*, 120−128.

(13) Garsany, Y.; Ge, J.; St-Pierre, J.; Rocheleau, R.; Swider-Lyons, K. E. Analytical Procedure for Accurate Comparison of Rotating Disk Electrode Results for the Oxygen Reduction Activity of Pt/C. *J. Electrochem. Soc.* **2014**, *161* (5), F628.

(14) Schmidt, T. J.; Gasteiger, H. A.; Stäb, G. D.; Urban, P. M.; Kolb, D. M.; Behm, R. J. Characterization of High-Surface-Area Electrocatalysts Using a Rotating Disk Electrode Configuration. *J. Electrochem. Soc.* **1998**, *145* (7), 2354−2358.

(15) Gloaguen, F.; Durand, R. Simulations of PEFC Cathodes: An Effectiveness Factor Approach. *J. Appl. Electrochem.* **1997**, *27* (9), 1029−1035.

(16) Herrero, E.; Buller, L. J.; Abruña, H. D. Underpotential Deposition at Single Crystal Surfaces of Au, Pt, Ag and Other Materials. *Chem. Rev.* **2001**, *101* (7), 1897−1930.

(17) Doña Rodríguez, J. M.; Herrera Melián, J. A.; Pérez Peña, J. Determination of the Real Surface Area of Pt Electrodes by Hydrogen Adsorption Using Cyclic Voltammetry. *J. Chem. Educ.* **2000**, *77* (9), 1195.

(18) Paulus, U. A.; Wokaun, A.; Scherer, G. G.; Schmidt, T. J.; Stamenkovic, V.; Markovic, N. M.; Ross, P. N. Oxygen Reduction on High Surface Area Pt-Based Alloy Catalysts in Comparison to Well Defined Smooth Bulk Alloy Electrodes. *Electrochim. Acta* **2002**, *47* (22), 3787−3798.

(19) Zhan, D.; Velmurugan, J.; Mirkin, M. V. Adsorption/Desorption of Hydrogen on Pt Nanoelectrodes: Evidence of Surface Diffusion and Spillover. *J. Am. Chem. Soc.* **2009**, *131* (41), 14756−14760.

(20) Trasatti, S. Development of the Work Function Approach to the Underpotential Deposition of Metals. Application to the Hydrogen Evolution Reaction*. *Z. Phys. Chem.* **1975**, *98* (1−6), 75−94.

(21) Łosiewicz, B.; Martin, M.; Lebouin, C.; Lasia, A. Kinetics of Hydrogen Underpotential Deposition at Ruthenium in Acidic Solutions. *J. Electroanal. Chem.* **2010**, *649* (1), 198−205.

(22) Kirowa-Eisner, E.; Bonfil, Y.; Tzur, D.; Gileadi, E. Thermodynamics and Kinetics of Upd of Lead on Polycrystalline Silver and Gold. *J. Electroanal. Chem.* **2003**, *552*, 171−183.

(23) Holewinski, A.; Idrobo, J.-C.; Linic, S. High-Performance Ag−Co Alloy Catalysts for Electrochemical Oxygen Reduction. *Nat. Chem.* **2014**, *6* (9), 828−834.

(24) Van Cleve, T.; Gibara, E.; Linic, S. Electrochemical Oxygen Reduction Reaction on Ag Nanoparticles of Different Shapes. *ChemCatChem* **2016**, *8* (1), 256−261.
(25) Green, C. L.; Kucernak, A. Determination of the Platinum and Ruthenium Surface Areas in Platinum−Ruthenium Alloy Electrocatalysts by Underpotential Deposition of Copper. I. Unsupported Catalysts. *J. Phys. Chem. B* **2002**, *106* (5), 1036−1047.
(26) Hachiya, T.; Honbo, H.; Itaya, K. Detailed Underpotential Deposition of Copper on Gold(III) in Aqueous Solutions. *J. Electroanal. Chem. Interfacial Electrochem.* **1991**, *315* (1), 275−291.
(27) Mayrhofer, K. J. J.; Strmcnik, D.; Blizanac, B. B.; Stamenkovic, V.; Arenz, M.; Markovic, N. M. Measurement of Oxygen Reduction Activities via the Rotating Disc Electrode Method: From Pt Model Surfaces to Carbon-Supported High Surface Area Catalysts. *Electrochim. Acta* **2008**, *53* (7), 3181−3188.
(28) Rudi, S.; Cui, C.; Gan, L.; Strasser, P. Comparative Study of the Electrocatalytically Active Surface Areas (ECSAs) of Pt Alloy Nanoparticles Evaluated by Hupd and CO-Stripping Voltammetry. *Electrocatalysis* **2014**, *5* (4), 408−418.
(29) Moniri, S.; Van Cleve, T.; Linic, S. Pitfalls and Best Practices in Measurements of the Electrochemical Surface Area of Platinum-Based Nanostructured Electro-Catalysts. *J. Catal.* **2017**, *345*, 1−10.
(30) Binninger, T.; Fabbri, E.; Kötz, R.; Schmidt, T. J. Determination of the Electrochemically Active Surface Area of Metal-Oxide Supported Platinum Catalyst. *J. Electrochem. Soc.* **2014**, *161* (3), H121−H128.
(31) Shao, M.; Odell, J. H.; Choi, S.-I.; Xia, Y. Electrochemical Surface Area Measurements of Platinum- and Palladium-Based Nanoparticles. *Electrochem. Commun.* **2013**, *31*, 46−48.
(32) van der Vliet, D. F.; Wang, C.; Li, D.; Paulikas, A. P.; Greeley, J.; Rankin, R. B.; Strmcnik, D.; Tripkovic, D.; Markovic, N. M.; Stamenkovic, V. R. Unique Electrochemical Adsorption Properties of Pt-Skin Surfaces. *Angew. Chem., Int. Ed.* **2012**, *51* (13), 3139−3142.
(33) Shao, M.; Chang, Q.; Dodelet, J.-P.; Chenitz, R. Recent Advances in Electrocatalysts for Oxygen Reduction Reaction. *Chem. Rev.* **2016**, *116* (6), 3594−3657.
(34) Strmcnik, D.; Tripkovic, D.; van der Vliet, D.; Stamenkovic, V.; Marković, N. M. Adsorption of Hydrogen on Pt(111) and Pt(100) Surfaces and Its Role in the HOR. *Electrochem. Commun.* **2008**, *10* (10), 1602−1605.
(35) Ochal, P.; Gomez de la Fuente, J. L.; Tsypkin, M.; Seland, F.; Sunde, S.; Muthuswamy, N.; Rønning, M.; Chen, D.; Garcia, S.; Alayoglu, S.; Eichhorn, B. CO Stripping as an Electrochemical Tool for Characterization of Ru@Pt Core-Shell Catalysts. *J. Electroanal. Chem.* **2011**, *655* (2), 140−146.
(36) Vidaković, T.; Christov, M.; Sundmacher, K. The Use of CO Stripping for in Situ Fuel Cell Catalyst Characterization. *Electrochim. Acta* **2007**, *52* (18), 5606−5613.
(37) Sugimoto, W.; Aoyama, K.; Kawaguchi, T.; Murakami, Y.; Takasu, Y. Kinetics of CH3OH Oxidation on PtRu/C Studied by Impedance and CO Stripping Voltammetry. *J. Electroanal. Chem.* **2005**, *576* (2), 215−221.
(38) Chatenet, M.; Soldo-Olivier, Y.; Chaînet, E.; Faure, R. Understanding CO-Stripping Mechanism from NiUPD/Pt(110) in View of the Measured Nickel Formal Partial Charge Number upon Underpotential Deposition on Platinum Surfaces in Sulphate Media. *Electrochim. Acta* **2007**, *53* (2), 369−376.

https://dx.doi.org/10.1021/acscatal.0c03028
ACS Catal. 2020, 10, 10735−10741